Manuscript Details

Manuscript number	EJPB_2017_602_R1
Title	Intermolecular interaction and solid state characterization of abietic acid/chitosan solid dispersions possessing antimicrobial and antioxidant properties.
Article type	Research Paper

Abstract

The aim of this work was to prepare and characterize solid dispersions of abietic acid (AB) and chitosan (CS) to investigate how formulation of the mixture may help in the battle against microbial colonization in different areas, such as the biomedical field or the food industry. Solid dispersions were characterized by differential scanning calorimetry, infrared spectroscopy, Raman spectroscopy, polarized optical microscopy, zeta potential and size analysis. The data showed that the dispersion/solvent evaporation method formed solid dispersions in which abietic acid was molecularly dispersed in the carrier. A synergistic effect between the two components in terms of antioxidant and antimicrobial properties was found, especially in the formulations obtained with 1/1 AB/CS molar ratio. Interestingly, the aggregation state (amorphous/crystalline) of AB seemed to affect the antimicrobial activity of the formulation, suggesting increased bioactivity when the drug was in the amorphous state. These findings, together with the demonstrated biocompatibility of the formulations, seem to open promising perspectives for a successful application of the developed AB/CS formulations in the biomedical field or in the food industry.

Keywords	Chitosan; abietic acid; solid dispersion; antimicrobial formulations; antioxidant formulations
Corresponding Author	Iolanda Francolini
Order of Authors	Valentina Cuzzucoli Crucitti, Luisa Maria Migneco, Antonella Piozzi, Vincenzo Taresco, Martin Garnett, Richard H. Argent, Iolanda Francolini
Suggested reviewers	Alexandra Muñoz-Bonilla, Birthe Veno Kjellerup, Fabiana Quaglia

Submission Files Included in this PDF

File Name [File Type]

Cover letter.docx [Cover Letter]

Responses to reviewers.docx [Response to Reviewers]

G.Abstract.tif [Graphical Abstract]

Paper.revised.docx [Manuscript File]

To view all the submission files, including those not included in the PDF, click on the manuscript title on your EVISE Homepage, then click 'Download zip file'.

To the Editor

European Journal of Pharmaceutics and Biopharmaceutics

Dear Prof. Nicolas Bertrand,

Thank you for considering our work for publication in European Journal of Pharmaceutics and Biopharmaceutics.

We have addressed the reviewer's comments and revised the manuscript accordingly. All revisions are in red in the manuscript.

I hope that now the manuscript is suitable for publication.

Kind regards,

Iolanda Francolini

Iolanda Francolini, PhD

Researcher

Dept. Chemistry - Sapienza University of Rome

Piazzale Aldo Moro, 5 - 00185 Rome, Italy

Tel. +39 06 49913162

Reviewer 1

This manuscript presents the comparison between two methods of mixing chitosan (CS) and abietic acid (AB). The first method is based on mechanical mixing, whereas the second method is based on dissolution. The two series of blending were characterized by DSC, IR, Raman and POM. Moreover, the antibacterial and antioxidant properties of those mixing were evaluated. The manuscript is well written and the language is good. However, several points are risen through this manuscript.

1) The major point is the characterization of the CS/abietic acid blends obtained by dissolution. Chitosan was first solubilized in acetic acid before to be mixed with abietic acid. Chitosan was protonated acetic acid and a solution of chitosan acetate was obtained. Chitosan acetate was further mixed with abietic acid and the resulting solution was freeze dried. No purification was realized. The content in acetate was not determined as well as the ratio of protonated and non-protonated abietic acid. The exact composition of these blends is not known and will depend of the experimental conditions. The lack of characterization affects the discussion through the manuscript. As example, what are the antibacterial properties of abietic acid, abietate and acetate ions?

We apologize to have left out the information about the purification of CS/AB blends during the description of their preparation. As correctly pointed out by the reviewer, the excess of acetic acid (used to solubilize CS) must be removed from the mixture because it may affect the properties of the resulting blends. We have, indeed, purified CS solution from the excess of acetic acid by dialysis before the abietic acid dispersion. We added these experimental details in the manuscript (Page 6 lines 119-127).
As for the antimicrobial properties of abietic acid and abietate, we have only determined the MIC of sodium abietate because abietic acid is not water soluble. This issue has been clarified in the manuscript (Page 8, line 171-172).
The antimicrobial activity of acetate ions was not tested. We believe that acetate content in the solution is very low since the excess was removed by dialysis. That is reflected in the high MIC value of the $(CS/AB)_{SD}$ 0.5/1 solid dispersion, situation in which we expect the highest release of acetate ions from CS since AB is in molar excess (exchange with abietate).

2) Comparison with literature of the glass transition temperature of chitosan should be discussed.

The discussion of CS glass transition temperature in the framework of the literature was added (Page 10 lines 235-238, Page 11 lines 239-240). Four references were also added [31-34].

3) The IR bands of abietic acid between 3000 and 2800 cm^{-1} are related to C-H stretching and not to O-H. O-H stretching bands for carboxylic acid are very broad from 3600 to 2200 cm^{-1}.

We agree with the reviewer. We changed the text and added a more in depth explanation of the abietic acid IR spectrum bands (see Page 11, lines 261-264) also with the help of new reference "V. Beltran et al. Anal. Bioanal. Chem. 408 (2016) 4073-4082".

The band at 1690 cm^{-1} is related to C=O stretching of carboxylic group. Where the C=O stretching band of carboxylate is observed? Carboxylate band should be at much more lower value.

The carboxylated band of abietic acid is, indeed, at lower value compared to C=O stretching of carboxylic group, that is 1554 cm^{-1} (Page 12 line 278).

Contrary to line 617, the deacetylated repeating units of chitosan also possess aliphatic moieties that adsorb about 2800-3000 cm^{-1}.

The mistake was corrected. Both deacetylated and acetylated units of chitosan contribute to the adsorption at 2800-3000 cm^{-1} (Page 12, line 267)

What is the assignation of the band at 1554 cm^{-1} ? This band was used in Fig 8. Quantification by ATR on solid sample is difficult to achieve due to the variation in contact between the sample and the probe. The authors did not mentioned if a calibration curve was performed. What is the accuracy on the A1554/A1690 ratio?

The band at 1554 cm^{-1} is related to the carboxylated abietic acid. The shifting of the peak of AB carboxylic acid from 1690 to 1554 cm^{-1} was considered an indication of the formation of a salt between AB and CS. The (1690/1554) intensity ratio was used to highlight a trend of the AB-CS salt formation with the increase in CS/AB molar ratio. The ratio gives just a qualitatively estimation of such phenomenon and is not an absolute value (Page 12, lines 285-286). The curves reported in Figure 8 can be considered calibration curves if used to estimate the composition of an unknown mixture.

4) The introduction section mentioned the importance of microbial biofilms, but all antibacterial experiments were realized in solution.

We revised the introduction to give less emphasis to the biofilm issue that was not faced in the experimental phase of this work. Future studies will be planned to test our blends towards *S. epidermidis* microbial biofilm in order to collect evidence on their activity vs sessile-growing bacteria.

5) Identification of curves in Fig. 4 and 6 is not clear.

We added markers on each curve to permit a clear identification of the samples.

-**Reviewer 2**

This manuscript details the development of antimicrobial compounds based on solid dispersions of abietic acid (AB) and chitosan (CS).

Comments:

1. The abstract states that these compounds also could be anti-biofilm compounds, however no evidence or results were shown throughout the manuscript and statements like this should be removed from the manuscript.

We removed in the abstract the concept of microbial biofilm and we focused on microbial colonization in general.

2. The text is well written, but there are MANY abbreviations and letter combinations that all together make it hard to follow and understand, since the reader must concentrate on this instead of understanding the science itself. Therefore I recommend that the authors revise the paper so the majority of these abbreviations/letter combinations are removed and the most important ones left behind.

We made an effort to reduce the number of abbreviations along the manuscript.

3. The figures are of poor quality and cannot be published as they appear. In particular Figures 4 and 6 are difficult to understand, since all the lines are black and the different styles do not differentiate. The rest of the figures appear pixelated.

We added markers on Figures 4 and 6 curve to permit a clear identification of the samples. We also improved the resolution of figures, where needed.

4. Figure 10 legend: "Comparison of the MIC values of (CS:AB)PM 1:1 and (CS/AB)SD 1:1.". The descriptions underneath the 2 bars in the graph do not reflect this.

For sake of clarity, Figure 10 and the description underneath the 2 bars have been changed.

5. Figure 9 - why are these figures in color?

Different colors were used only to permit a good identification of the samples.

6. Figure 2. The microscopic images should be explained in more detail in the legend as well. It is really hard to see anything in panel C. Should it be removed?

In the capture of Figure 2, explanation of the POM images concerning the crystalline or amorphous state of the drug have been included. We believe that Panel C is needed because is the only image showing the amorphous state of the drug (no birifrangence).

7. Table 4: The concentrations should be added as a column in this table. It is not enough to say "2 x MIC".

As suggested, the concentrations have been added in Table 4

8. References: Bacterial names must be italicized. Other spelling mistakes should also be corrected.

Done

9. Conclusions: This was stated: "It is difficult to be sure of the effects of the various parameters.". Please revise this statement and other in the conclusion, so you write what it IS that you can say and what you can conclude does not occur. The conclusion must be stronger and based on the results in the paper. Other wise it must be characterized as Future experiments.

As suggested, Conclusions were rewritten to highlight the significant results obtained in the work.

10. The authors claim that the AB and CS compounds are antimicrobial. Limited experimental results have been shown to support this and none of these were referred to in the conclusion. I recommend that the authors revise the manuscript to reflect that they are interested in "antimicrobial properties" and not only the chemical characteristics and whether they dissolve or form solids. This should be discussed in the context of how and why this would make the compounds more/less antimicrobial.

The introduction was revised to reflect the real goal of the work, that is the development of formulations with improved antimicrobial activity.

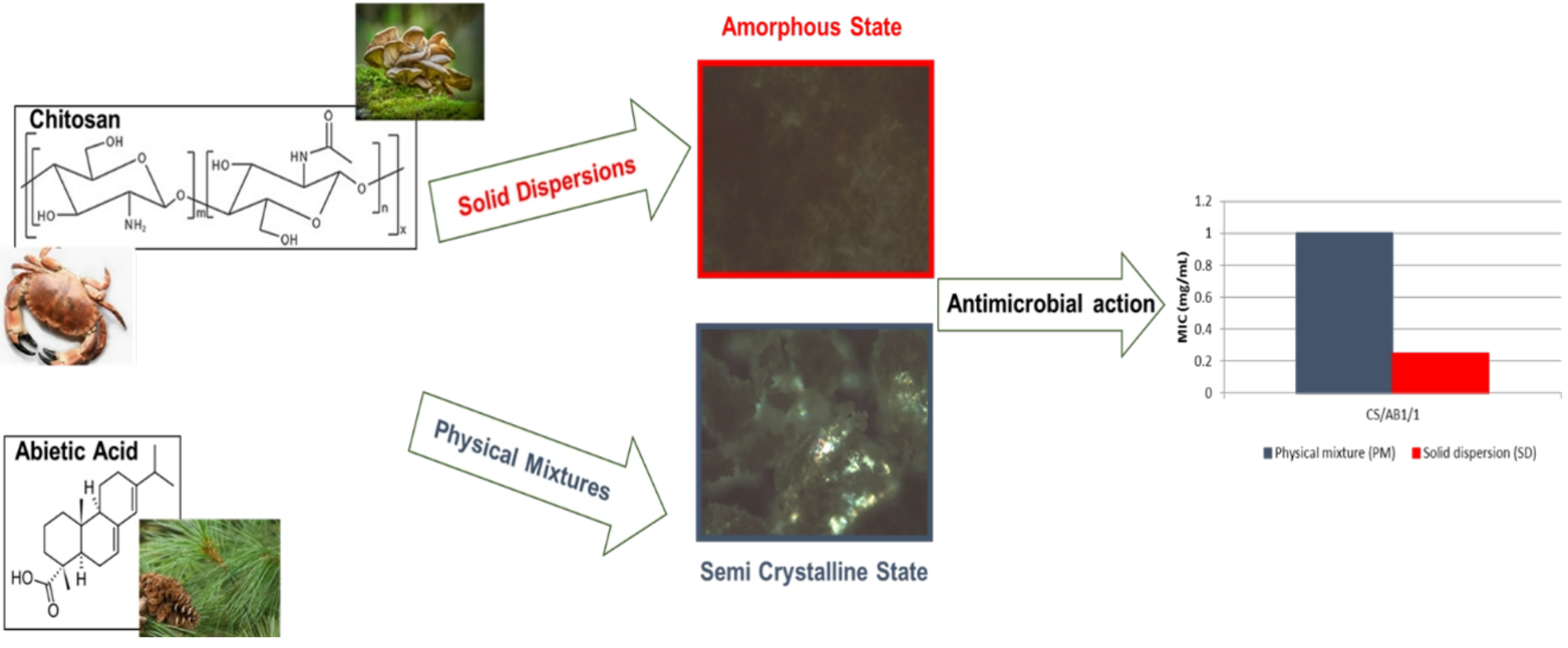
Chitosan
Abietic Acid
Solid Dispersions
Physical Mixtures
Amorphous State
Semi Crystalline State
Antimicrobial action
MIC (mg/mL)
1.2
1
0.8
0.6
0.4
0.2
0
CS/AB1/1
Physical mixture (PM)
Solid dispersion (SD)

Intermolecular interaction and solid state characterization of abietic acid/chitosan solid dispersions possessing antimicrobial and antioxidant properties.

Valentina Cuzzucoli Crucitti[a,1], Luisa Maria Migneco[a], Antonella Piozzi[a], Vincenzo Taresco[b], Martin Garnett[b], Richard H. Argent[b], Iolanda Francolini[a]*

[a] Sapienza University of Rome, Department of Chemistry, Rome, Italy.

[b] School of Pharmacy, University of Nottingham, Nottingham, NG7 2RD, UK.

[1] Department of Chemical and Environmental Engineering, Faculty of Engineering, University of Nottingham, Nottingham, NG7 2RD, UK. (Present Address of Valentina Cuzzucoli Crucitti)

Corresponding author: Iolanda Francolini

Sapienza University of Rome

Department of Chemistry

Piazzale Aldo Moro 5, 00185 - Rome, Italy

Tel. +39 06 4991 3162

Fax. +39 064991 3692

E-mail: iolanda.francolini@uniroma1.it

Abstract

The aim of this work was to prepare and characterize solid dispersions of abietic acid (AB) and chitosan (CS) to investigate how formulation of the mixture may help in the battle against microbial colonization in different areas, such as the biomedical field or the food industry. Solid dispersions were characterized by differential scanning calorimetry, infrared spectroscopy, Raman spectroscopy, polarized optical microscopy, zeta potential and size analysis. The data showed that the dispersion/solvent evaporation method formed solid dispersions in which abietic acid was molecularly dispersed in the carrier. A synergistic effect between the two components in terms of antioxidant and antimicrobial properties was found, especially in the formulations obtained with 1/1 AB/CS molar ratio. Interestingly, the aggregation state (amorphous/crystalline) of AB seemed to affect the antimicrobial activity of the formulation, suggesting increased bioactivity when the drug was in the amorphous state. These findings, together with the demonstrated biocompatibility of the formulations, seem to open promising perspectives for a successful application of the developed AB/CS formulations in the biomedical field or in the food industry.

Keywords

Chitosan; abietic acid; solid dispersion; antimicrobial formulations; antioxidant formulations

Introduction

~~Microbial biofilms are defined as microbial populations irreversibly attached to a surface, embedded in an extracellular matrix, mainly composed of polysaccharides, produced by the microorganisms themselves [1]. The advantages of this highly cooperative community are mostly to do with survival, since microorganisms in biofilms are up to 1000-times more resistant to antibiotics with respect to their planktonic counterparts [2]. The ability of many microbial species to form biofilms has important implications in various sectors, especially in the biomedical field [3,4] and in the food industry [5,6].~~

~~Due to the emergence of antibiotic-resistant microorganisms, t~~The understanding of mechanisms by which living organisms defend themselves from invasion by pathogens has become a major source of inspiration for the development of new antimicrobial formulations particularly for finding solutions to the emergence of antibiotic-resistant microorganisms [1,2]. Similarly there has been increased interest in natural antimicrobial agents. In the last decade, chitosan (CS) has been recognized as a versatile antimicrobial agent displaying excellent biocompatibility, physical stability and processability [3]. In the food industry, chitosan is used as a preservative for improvement of quality and shelf life of foods [4] and can be either added in the food or applied to the surface to provide an edible protective coating [5]. In the biomedical field, chitosan is mainly used for drug/gene delivery [6]. Recently, to improve its antimicrobial activity, chitosan has been blended with different antimicrobial agents including antibiotics [7,8] and natural antimicrobial extracts [9,10]. Plants are known to be able to produce a variety of small antimicrobial molecules (MW <500 g/mol), generally classified as "phytoalexins", among which the most common belong to the classes of glycosteroids, flavonoids, terpenes, di-terpenes, terpenoids and polyphenols [11,12]. In this framework, the di-terpene abietic acid (AB) has been recently recognized as a substance with important biological activities [13]. Abietic acid is the major component of rosin that is the non-volatile portion of the resin produced mostly by conifers [14]. The production of

such resin is associated with a defense mechanism against attack by insects or fungal infections in presence of a tissue injury and that in part explains why AB possesses antimicrobial activity against some Gram-positive bacteria, including *Staphylococcus aureus*, one of the most important pathogenic bacteria [15]. That has prompted research into potential applications as an antibacterial agent [16-18].

A limiting factor in the application of AB is its poor solubility in an aqueous environment resulting from the strong hydrophobicity of the hydrophenanthrene skeleton (Fig. 1a).To increase AB water solubility, AB has been either functionalized with quaternary ammonium groups or linked to hydrophilic polymers [19]. Acrylic and methacrylic polymers based on AB have also been synthesized [19] from monomers obtained by reaction of AB with hydroxyl ethyl methacrylate, hydroxyl ethyl acrylate and hydroxyl ethyl butyl acrylate. Although these strategies have had some benefits, they can be time consuming and expensive.

In this work, for the first time, ~~antimicrobial~~ solid mixtures based on abietic acid and chitosan were developed and characterized in order to improve AB water solubility and produce antimicrobial formulations with improved activity compared to pure components. The hypothesis is that the hydrophilic chitosan may interact with AB, reduce the size of drug particles, change the drug crystalline state and increase drug wettability. Indeed, CS possesses amine groups (Fig. 1b) potentially involved in acid/base interaction with the AB carboxylic group, thus favoring the intimate interaction between the drug and the carrier [20]. In the whole, the interaction between CS and AB could increase availability of the drug and its antimicrobial efficacy towards microrganisms. Additionally, being CS intrinsically antimicrobial, CS could have the dual function of allowing AB dissolution and to explicate a biocidal action as the same time as AB. That is of course beneficial for increasing the chances of success of the formulation and reducing the risk of selecting drug resistant microrganisms.

In order to find out the best condition promoting CS/AB interaction, different CS/AB molar ratios and different preparation methods were investigated. The resulting systems were

characterized by IR and Raman spectroscopy, differential scanning calorimetry, polarized optical microscopy, zeta potential and size analysis. The biological properties of the formulations were also evaluated. Particularly, the antimicrobial activity was determined versus a reference strain of *Staphylococcus epidermidis,* chosen because of its involvement in numerous nosocomial infections, such as wound infections and medical device-related infections. The antioxidant property of CS/AB formulations was also determined. This feature, in combination with the antimicrobial one, may be relevant since free radicals, produced during the inflammatory response of the body to a pathogen, have been shown to favor diversity and adaptability in biofilm communities [21]. Finally, a hemolysis test was performed.

2. Experimental part

2.1 Materials and Methods

Chitosan (CS, deacetylated 85%, low molecular weight) was obtained from Sigma-Aldrich. Abietic Acid (AB, 85%) was supplied by Acros Organics. 2,2 diphenyl-1-picrylhydrazyl radical (DPPH), sodium hydroxide, acetic acid, methanol were purchased from Sigma-Aldrich. The regenerated cellulose membrane (Spectrapor membrane BIOTECH) had a cut-off of 3500 Da. The Gram-positive *Staphylococcus epidermidis* ATCC 35984, grown in Muller Hinton (MH, Oxoid) medium, was employed for the microbiologic tests.

2.2 Preparation of drug-polymer solid mixtures

Drug-polymer solid mixtures were prepared by incorporating AB within CS in varying molar ratios(CS:AB 0.5:1, 1:1, 2:1, 4:1 and 6:1), corresponding to AB weight percentages equal to 80%, 65%, 50%, 33% and 25%. Two methods were used for preparation of drug-polymer mixtures: (i)

physical mixing of the powders by grinding them in a mortar for about 10 min and (ii) dispersion of the drug in a water solution of protonated CS. In this latter method, the following procedure was used. First, CS was solubilized in an aqueous solution of 1% acetic acid. Subsequently, the solution was dialyzed against DI water, using a cellulose membrane with a 3500 Da cut-off, and the protonated CS was recovered by freeze-drying and re-dissolved in water. AB was dispersed to this latter solution using the desired amount according to the targeted molar ratio.~~in 1% acetic acid followed by lyophilization~~. The formulations obtained with the first method were named as $(CS:AB)_{PM}$ while the second ones as $(CS:AB)_{SD}$, where the subscript PM stands for physical mixture and SD for solid dispersion. All the dispersions were left stirring overnight in order to get an intimate drug:polymer interaction.

2.3 Characterization of drug-polymer solid mixtures

Infrared analysis in attenuated total reflection (IR-ATR) was accomplished by using a Thermo Nicolet 6700 instrument equipped with a Golden Gate diamond single reflection device (Specac). Spectra were acquired at a resolution of 2 cm^{-1}, in the range 4000–650 cm^{-1}.Differential Scanning Calorimetry (DSC) was performed using a METTLER TA-3000calorimeter with3-5 mg of sample, in the 25-250°C temperature interval, at a heating rate of 10K/min, under nitrogen.

The electrophoretic mobility was measured by the electrophoretic laser Doppler technique using a NanoZetaSizer (Malvern, UK) equipped with a 5 mWHeNe laser. The zeta potential of the particles was obtained from the measurement of mobility ν, by using the Smoluchowski equation:

$$\nu = 4\pi\varepsilon_0\varepsilon_r\frac{\xi}{6\pi\mu}(1 + kr)$$

where ε_0 and ε_r are the relative dielectric constant and the electrical permittivity of a vacuum, respectively, μ is the solution viscosity, r is the particle radius, and k is the Debye–Hückel parameter defined as:

$$k = \sqrt{\frac{2n_0 z^2 e^2}{\varepsilon_0 \varepsilon_r k_B T}}$$

where n_0 is the bulk ionic concentration, z is the valence of the ion, e is the charge of an electron, k_B is the Boltzmann constant, and T is the absolute temperature.

An advanced Polarising Optical Microscope (POM, HS1 microscope), Prior Lux POLTM with 12V and 30W halogen lamp with variable brightness control, was employed to analyze the crystalline state of the drug in the different drug-polymer mixtures.

UV–Vis spectra were obtained by using a HP U2000 singular beam spectrophotometer working in the 190–1100 nm wavelength range and with a resolution of 0.004 nm.

A confocal spectroscopy system (Horiba-Jobin-Yvon Ltd, Middlesex, UK) was used to collect Raman spectra of raw materials and the drug-polymer formulations, in the wavelength range of 40-1800 cm^{-1}. The experiments were performed with a near-IR laser (785 nm) of 250 mW power. Spectra were acquired using a 50× objective and a 300 μm confocal hole. A 600 lines/mm rotatable diffraction grating was used to simultaneously scan a range of frequencies.

2.4 Evaluation of the antioxidant activity of the CS:AB solid mixtures

The antioxidant activity of the solid mixtures was determined by using DPPH as a free anionic radical [22]. For each sample, different concentrations were tested (expressed as the molar ratio between the antioxidant agent, in our case AB, and DPPH). Firstly, a 0.2 M MDPPH stock solution in methanol was prepared. Then, an aliquot of this solution (2 ml) was added to an acetic acid solution (1%, 2 ml) containing the different CS:AB solid mixtures at varying concentrations. CS and AB were also tested alone as control samples. The variation in absorbance was determined at room temperature at 520 nm after 30 min. The amount of residual DPPH was evaluated from a previously obtained calibration curve at the same wavelength. The antioxidant activity of each solid mixture was expressed in terms of Effective Concentration (EC_{50}), which is the amount of

antioxidant agent necessary to decrease the initial DPPH concentration by 50%.EC_{50} values were extrapolated from a graph obtained by plotting the residual DPPH as a function of antioxidant agent:DPPH molar ratio.

2.5 Evaluation of the antimicrobial activity of the CS:AB solid mixtures

The antibacterial activity of the CS:AB solid mixtures was assessed against *S. epidermidis*. The minimum inhibitory concentration (MIC) of each sample was determined as previously described [23]. The activity of pure CS and AB was also evaluated, as controls. Specifically, due to AB insolubility in water, the MIC of sodium abietate was determined. Briefly, a bacterial inoculum at 1×10^6 CFU/ml in tryptic soy broth (TSB) with an optical density of 0.05 at 550 nm was first prepared. Subsequently, sample (1 ml)at various concentrations was added to test tubes containing bacterial inoculum (1 ml). A control tube containing bacterial inoculum and TSB was also prepared. Control and test tubes were incubated at 37°C for 24 h. Following incubation, bacterial growth was determined by measuring the absorbance at 550 nm and the percentage of bacterial inhibition (I%) was calculated as follows:

$$I\% = 1 - \frac{A_S - A_0}{A_{control} - A_0} * 100$$

where A_0 is the absorbance of the inoculum before incubation, $A_{control}$ is the absorbance of the inoculum after incubation and A_s is the absorbance of the sample after incubation. All the experiments were performed in triplicate. Differences were considered significant for $P < 0.05$.

2.6 Evaluation of the haemolytic activity of the solid mixtures

For the hemolysis assay, blood was collected into heparinised tubes and erythrocytes harvested and washed in Phosphate-Buffered Saline (PBS) as described [24]. The pure materials and CS:AB solid mixtures were diluted in PBS (100 µl) and added to 48-well plates followed by erythrocyte suspension (150 µl) and incubated for 1 h at 37°C, before centrifugation at 500 rpm for 5 min. Supernatant (100 µl) was carefully transferred to a clear 96-well plate and release of hemoglobin determined using a TECAN Spark 10M plate reader at 450 nm. PBS was used as the negative (no lysis) control and 0.2% Triton X-100 used as the positive (complete lysis) control, and percentage hemolysis was calculated relative to these controls:

$$\%Hemolysis = \frac{(Abs_{test} - Abs_{PBS})}{(Abs_{TX} - Abs_{PBS})} * 100$$

3. Results and discussion

Several methods have been employed in the literature for the preparation of drug-polymer solid mixtures [25] in the formulation of water-insoluble drugs, among which the commonest are:(i) the physical mixing of the drug and polymer powders, and (ii) the dispersion of the drug into a polymer solution. These methods are simple and can be used for all kinds of drugs, even thermolabile ones, since the drugs do not need special treatments.

When developing drug-polymer solid mixtures, it is interesting to understand if the drug is molecularly dispersed (or not) in the polymer carrier since this condition is usually associated with a better drug solubility. Due to the complexity of the drug-polymer intermolecular interactions, it is not always trivial to delineate the differences between molecularly dispersed and not molecularly dispersed solid mixtures. In the case of drugs which are capable of crystallization, a formulation lacking ordered crystalline structures, is commonly considered as a molecularly dispersed mixture [26,27].In the present work, to evaluate the level of drug-polymer interaction in the solid mixtures

different analytical techniques were employed, namely POM,FT-IR, Raman spectroscopy and DSC analysis [28,29].

POM observation of the solid mixtures

The observations of the samples by POM were conducted to evaluate the state (crystalline or amorphous) of the drug, qualitatively and rapidly in different solid mixtures. Indeed, the observation of birefringence indicates the presence of a crystalline phase. AB alone is a crystalline compound as shown in Figure 2A. When AB is physically mixed with CS in any of the employed molar ratios, it keeps crystallinity, at least in part, as shown in Figure 2B where the POM image obtained for $(CS:AB)_{PM}$ 1:1 is reported. On the contrary, the $(CS:AB)_{SD}$ mixtures, obtained by drug dispersion in the polymer solution, did not show any birefringence for all CS:AB molar ratios equal to or greater than 1:1 (Fig.2C), suggesting a good drug-polymer interaction for these samples.

Differential scanning calorimetry

In solid drug-polymer systems, either the decrease, shift or disappearance of the endothermic peak usually indicates that the drug is present in an amorphous state rather than its crystalline form, or in an amorphous-latex mixture [29]. In Figure 3, the thermograms of pure AB and CS are reported. In the AB thermogram (Fig. 3A), an exothermic band at about 160°C is followed by an endothermic peak at 168°C indicating an initial partial drug crystallization during the DSC experiment followed by the melting of the whole crystalline phase. The enthalpy of melting (ΔH_m) was found to be 36.8 J/g. The CS thermogram in the first scan (Fig. 3B) shows a wide endothermic band centered at about 100°C likely due to the presence of water. In the second cycle, however, a step at 116°C is observed relative to the glass transition of the amorphous portion of the polymer.The observation of this transition by DSC is not always easy to observe due to the rigidity

of CS that involves a low free volume associated with the chains [30]. The CS T_g value can be influenced by different factors such as crystallinity, molar mass, and degree of de-acetylation, as well as by the source and method of extraction. Different T_g values are, therefore, reported in the literature. Dhawade et al. [31] and Rotta et al. [32] obtained T_g values around 115 °C by DSC measurements while higher values (150-160 °C) were obtained by the dynamic mechanical analysis (DMA) [33,34].

The DSC thermograms of the$(CS:AB)_{PM}$ 1:1, 2:1, 4:1 and 6:1 samples are reported in Figure 4 in comparison to AB, in the temperature range of interest. Each thermogram was normalized as a function of the AB content and by keeping constant the total weight of each sample to 5 mg.

A progressive decrease of the AB melting peak with increasing CS:AB molar ratio was observed. This trend is evident if the enthalpy of melting of each sample, normalized for the AB content in the sample, is reported as a function of the CS:AB molar ratio (Fig.5). This finding indicates the occurrence of drug-polymer interactions that hinder drug crystallization. The interactions are especially promoted for high CS contents ($(CS:AB)_{PM}$ 4:1 and 6:1). A decrease in the melting temperature (T_m) with the increase of the CS:AB molar ratio was also observed, further underlining the presence of drug crystals with reduced order as a result of the interaction with CS.

As expected, the CS:AB interactions were more pronounced in the solid dispersions. Indeed, in these samples the drug was present substantially in the amorphous state in all the $(CS:AB)_{SD}$ ratios, and in the DSC thermogram an endothermic band rather than a sharp drug melting peak was observed (Fig. 6). This finding was in accordance with POM observations that showed the absence of birefringence associated with the crystalline state of the drug in all of the $(CS:AB)_{SD}$ ratios.

FT-IR Spectroscopy

FT-IR measurements were used to estimate the type and extent of drug-polymer interactions. In Fig. 7, the FT-IR spectra of AB, CS, $(CS:AB)_{PM}$ and $(CS:AB)_{SD}$ are reported. The IR spectrum of

AB (Fig. 7A) shows a large band at 3400 cm^{-1} and the two bands at 2650 and 2534 cm^{-1} correspond to the group –COOH [35]. Specifically, the first band to free OH and the last two to bonded OH related to the formation of dimers in the solid state. The C–H stretching absorption bands in the 3000-2800 cm^{-1} spectrum range. The band at 1690 cm^{-1} is related to the stretching of C = O. In the IR spectrum of CS (Fig 7B),the absorption related to the OH and NH stretching are present in the range between 3750 and 3000 cm^{-1}, while the absorption peak of the aliphatic moieties ~~, related to the fraction of acetylated CS,~~ is present at about 2800 cm^{-1}. The absorptions at 1645 and 1590 cm^{-1} correspond to the C = O stretching of the secondary amide of acetylated repeating units (amide I) and the NH bending of the secondary amine of residues of chitin, respectively. The stretching C-O-H and C-O-C are in the range between 1150 and 1000 cm^{-1}.

In the IR spectra of the $(CS:AB)_{PM}$ formulations (Fig. 7C), the presence of the two components in the formulations was confirmed by the absorption at 1690 cm^{-1}, related to the AB carbonyl group, and at ca. 1100 cm^{-1}, related to the chitosan C-O-H and C-O-C stretching. No significant shifting of the bands at all the CS:AB ratios was observed.

In contrast, important changes in specific absorption bands were observed in the IR spectra of the $(CS:AB)_{SD}$ formulations (Fig. 7D). Specifically, a significant reduction in the absorbance of the peak at 1690 cm^{-1}, related to the AB carboxylic acid group, accompanied by a corresponding increase in the absorbance of the peak at 1554 cm^{-1} (carboxylate C=O of AB) was observed as the CS content in the formulation increased. The shifting of the peak of AB carboxylic acid from 1690 to 1554 cm^{-1} is likely to be attributed to the formation of a salt between AB and CS by electrostatic (acid/base) interactions.

To qualitatively estimate the magnitude of the electrostatic drug-polymer interactions as a function of CS:AB molar ratio, the ratio between the absorbance of the peak at 1554 $cm^{-1}(A_{1554})$ and that of the peak at1690 $cm^{-1}(A_{1690})$ was plotted vs CS:AB molar ratio for both series of samples (Fig. 8). The $\frac{A_{1554}}{A_{1690}}$ ratio is a relative value, not an absolute parameter, and was used to highlight the

trend of the CS-AB salt formation with variation in CS:AB molar ratio. Only for the $(CS:AB)_{SD}$ samples a significant increase of the $\frac{A_{1554}}{A_{1690}}$ ratiowas observed, suggesting that CS:AB interactions were promoted by the increase of CS:AB ratio.

Raman spectroscopy

In order to have a better insight into the AB level of structural interaction in the formulations and to reinforce the POM, IR and DSC observations, Raman spectroscopy analysis was carried out on some selected samples. Particularly, this technique allowed evaluation of the presence of drug crystals or their different polymorphs (Raman phonon-region) [36]. Indeed, the phonon region pattern of crystalline forms, generally, presents defined peaks, while amorphous materials are characterized by broad features [37]. As shown in Figure9A and9B, AB Raman spectrum presents a precise pattern in the range between 40 and 400 cm^{-1}. On the contrary, CS does not show any peaks in this region. In Figure9A,the Raman traces of $(CS:AB)_{PM}$ samples are compared to AB and CS. The phonon regions show the same patterns which are weakened as the CS/AB ratio increased, confirming a crystalline AB order throughout the physical formulations. Moreover, observing the whole range of wave number (from 40 to 1800 cm^{-1}) all the formulations, apart from $(CS:AB)_{PM}$6:1, show the same pattern as AB alone with sharp and well-defined peaks. A less defined Raman spectrum can explain the reduction in crystallinity of AB in the $(CS:AB)_{PM}$6:1 mixture and it is in agreement with the DSC observations. As for the $(CS:AB)_{SD}$ samples, only the phonon region of $(CS:AB)_{SD}$ 1:1 (Fig. 9B) shows the same pattern as free AB, likely due to a partial re-crystallization of the drug in the blend. This possible AB order was not detected by DSC. Instead, $(CS:AB)_{SD}$ 2:1and $(CS:AB)_{SD}$ 6:1 samples do not show any peaks in the AB phonon region, suggesting the complete lack of order and thus drug amorphization in the formulations. This latter evidence

supports the lack of birefringence of those samples and lack of thermodynamic activity in the DSC traces.

Bioactivity of the formulations

On the basis of the results of the formulation physical characterization, the biological tests were performed only on the solid dispersions because in these samples, unlike the physical mixtures, the abietic acid was molecularly dispersed in the polymer carrier. It is, therefore, reasonable to assume that the solid dispersions can show better performance than the physical mixtures. Amongst the investigated CS:AB ratios, the 0.5:1, 1:1 and 6:1 samples were chosen in order to investigate the effects on the biological properties of CS being equimolar, in deficit or in large excess with respect to AB.

Antioxidant activity of the formulations

An inflammation process is often concomitant with the infectious disease. This process causes an oxidative stress that seems to have some effects on the course of the infection. In general, the role of free radicals in infections is two-fold. On one hand, free radicals protect against invading microorganisms. On the other hand, they can accumulate during the infection disease, cause tissue damage and, sometimes, have fatal consequences. Though specific experiments on the effects of oxidative stress on the severity of infections have not been carried out yet, some authors claim that the mitigation of oxidative stress using exogenous compounds appears to be a suitable complementary approach to treat infections [38]. Free radicals have been also shown to promote antibiotic resistance in biofilm-growing bacteria, as recently demonstrated in different biofilm communities [21]. Specifically, in cystic fibrosis patients the oxidative stress was shown to be associated with the occurrence of antibiotic resistant bacteria in the lung [39]. In addition, in an

animal model of wound infection, Dhall et al. reported on the role of high levels of reactive oxygen species (ROS) in establishment of chronic wounds [40,41]. Consequently a reduction in oxidative stress during antibacterial therapy would be an advantage.

To evaluate a possible antioxidant activity of the formulations, DPPH was used as the model free anionic radical and the activity was expressed in terms of EC_{50} and compared to the raw materials (Table 1). As expected, CS has a low antioxidant activity showing an EC_{50} of about 11 mg/ml, in agreement with literature data [42]. In contrast, AB showed a higher antioxidant activity, with an EC_{50} value of 1.65 mg/ml (5.4 x 10^{-3} M), even if less effective than common antioxidant polyphenols [43].

Looking at Table 1, for the SD formulations we can see that there is an inconsistency in the apparent EC_{50} for the formulations and their components in that two of the EC50 occur at a lower concentration, than we may expect. The relative contribution of each of the components is also unclear. However, if we calculate the amount of each component (CS and AB) present in the assay at the amount of EC_{50}, a clearer picture emerges. We can see that the concentration of AB component at the EC_{50} is similar (range 0.40-0.60 mg/mL) in all of the formulations and has a value that is about one quarter the EC_{50} of the pure AB. Considering the CS component, for the 0.5:1 and 1:1 CS/AB formulations the CS component is less than 2% of the EC50 and so unlikely to contribute significantly to antioxidant activity by its usual mechanism, but in the 6:1 formulation where it is 20% of the EC50 there may be some CS contribution. Overall therefore it seems that the presence of AB in the amorphous form is a more effective antioxidant.

There are a number of aspects which may account for this formulation advantage some of which may depend on the mechanism of the AB antioxidant activity. The antioxidant activity seems to be related solely, to the double bonds [44], with a proposed mechanism providing two alternative oxidative pathways, which can occur individually or simultaneously [44]. One pathway sees the production of an epoxy structure, the other one, instead, involves the production of peroxides and

free radicals [44]. Some authors have synthesized a catechol-derived AB to increase the antioxidant activity [45].

For the formulations, firstly, the amorphous versus the crystalline nature of the drug may have some effect in terms of solubility and availability of drug. Secondly, it is possible that a stabilization of the radical form of AB occurred thanks to interaction with CS. In fact, it is known that the AB radical is unstable and reacts with oxygen to form peroxides. Such oxidation is the cause of the bitter taste that can result from chewing gum which has 90 % of ester compounds made of AB [43], for a prolonged time. Usually, to avoid this oxidation, a second antioxidant, α-tocopherol, is added in the chewing gum which decreases peroxide levels and thus the AB degradation leading to the sensory perception. Therefore, in the formulations, chitosan may act similarly to α-tocopherol, stabilizing the AB radical.

Antimicrobial activity

To evaluate the effect of the new drug-polymer formulations on antibacterial activity compared to the raw materials, a broth dilution assay was performed using *S. epidermidis* as the model microorganism. MICs of both AB and CS were determined to be 0.8 and 0.5 mg/ml, respectively. The activity of CS is related to the presence of partially protonated NH_2 that can interact with the anionic bacterial cell membrane [46]. The AB activity is mainly attributable to the carboxylic functionality, which interacts with the lipid component of the bacterial cellular membrane allowing this molecule to penetrate inside the membrane, altering the membrane functions [47].

A preliminary screening of the antimicrobial activity of $(CS:AB)_{SD}$ and $(CS:AB)_{PM}$ 1/1 formulations was performed (Fig. 10) to assess whether the state of AB (amorphous or crystalline) might influence the antimicrobial activity. As determined from the physical-chemical characterization of the formulations, the state of AB in the two formulations tends to be partially crystalline in the $(CS/AB)_{PM}$1:1 while is completely amorphous in the $(CS/AB)_{SD}$ 1:1, so this state may affect the

solubility and thus the bioactivity. As can be observed in Figure 10, the physical mixture $(CS:AB)_{PM}$ 1:1 showed a MIC of 1 mg/mL significantly higher than $(CS:AB)_{SD}$ 1:1 (0.25 mg/ml), suggesting that the amorphicity or dispersion state of the drug may significantly affect the bioactivity of the drug itself.

To shedlight on the low value of MIC of $(CS:AB)_{SD}$ 1:1 in Figure 11, the percentage of bacterial inhibition (I%), defined as described in Materials and Methods, is reported as a function of component concentration for $(CS:AB)_{SD}$ 0.5:1, $(CS/AB)_{SD}$ 1:1 and $(CS/AB)_{SD}$ 6:1. The biological tests showed that the MIC values (i.e. the first concentration for which there was complete inhibition of bacterial growth)varied with the CS:AB molar ratio. When CS was in a molar excess with respect to AB, the sample $(CS:AB)_{SD}$ 6:1,the CS concentration in the formulation exceeded the CS MIC value (Table 2), so this result would be as predicted. Similarly, when CS was in a molar deficit with respect to AB, i.e. in the sample $(CS:AB)_{SD}$ 0.5:1, the formulation showed antimicrobial activity at 1 mg/ml (Fig. 11), that is when the AB component is at its MIC (Table 2). The most interesting situation was found in the formulation$(CS:AB)_{SD}$ 1:1. In this case, the MIC of the formulation was equal to 0.25 mg/ml, where both CS and AB were at concentrations below the MICs of either CS or AB alone, and below that which may be expected for an additive effect(Table 2). This finding strongly suggests a synergistic effect between the two components.

To understand reasons behind this synergy, size and zeta potential of the formulations were determined (Table 3), since these two features may influence the nanoparticle/bacteria interaction. In general, small nanoparticulate size and positive charge promote interaction with cells [48]. In our case, sizes and PDI values decreased as AB content increased. In particular, a reduction in average sizes and a narrower size distribution were observed with AB excess. This probably results from the polymer being involved in ionic interactions with AB as suggested from the change in zeta potential data. The decrease of repulsive interactions between the CS chains, and the presence of hydrophobic interactions probably most likely amongst AB rings is likely to lead to a compaction of aggregates to a state more like a defined nanoparticle. The near neutrality of the 1:1 complex might

be a further demonstration of the equimolar ratio of the two molecules. The complex 0.5:1, where AB is in a molar excess, showed a negative Zeta Potential. In contrast, the 6:1 complex is positively charged due to the large molar excess of CS.

It would be expected that the net negative charge may interfere with the binding of the CS/AB0.5:1 formulation to the bacterial cells, and that this may reduce the effectiveness of this formulation. However, the AB content is equivalent to the MIC of AB, so this component appears to have retained its normal effectiveness.

More difficult is to find an explanation for why $(CS/AB)_{SD}$ 1:1 had higher activity than $(CS/AB)_{SD}$6:1. Indeed, from size and charge data, we would have expected a better activity for $(CS/AB)_{SD}$ 6:1 that has a size similar to $CS/AB)_{SD}$ 1:1 (370 vs 440 nm) but a positive charge, unlike the $(CS/AB)_{SD}$ 1:1 that is essentially neutral (zeta potential = -5). Indeed, the positive charge of $(CS/AB)_{SD}$ 6/1 should confer this formulation with a higher binding ability towards the bacterial cell membrane and, therefore, with an antimicrobial activity higher than that of the $(CS/AB)_{SD}$ 1/1 formulation. Additionally, with the charges balanced between CS and AB, we may expect that this would affect the ability of each component to act by its normal mechanism through these charges being less available. To explain this odd behavior, we have called into question the role of the hydrophylic/hydrophobic balance on the antimicrobial activity of polymer formulations. It is known that the activity of cationic polymers is also related to the balance between cationic and hydrophobic moieties. Specifically, hydrophobic moieties can improve polymer activity since they promote the insertion of the polymer chain in the lipid bilayer of the cell membrane [49]. Therefore, it's reasonable to hypothesize that the neutral $(CS:AB)_{SD}$ 1:1 formulation possesses a suitable hydrophylic/hydrophobic balance that causes the disruption of the bacterial membrane not primarily by establishing electrostatic interactions with the membrane but mainly by insertion of the AB hydrophenanthrene ring (and maybe also of the polymer chain) into the lipid bilayer.

Hemolysis assay

To determine the biocompatibility of the most promising formulation, $(CS:AB)_{SD}$ 1:1, a hemolytic assay was carried out. The hemolysis activity of this sample was compared to that of CS, AB and $(CS:AB)_{PM}$1:1 formulation. For each sample, the test was performed at the MIC, below the MIC (0.25*MIC) and above the MIC (5*MIC). The two tested formulations as well as pure CS and AB showed negligible lytic activity (Table 4). This activity was lower than 1%, in the concentration range of 0.25*MIC up to 5*MIC for each formulation, indicating that the formulations presented have good biocompatibility.

Conclusions

Solid mixtures based on AB and CS were developed in order to produce antimicrobial formulations with improved activity. Results obtained by IR spectroscopy, thermal and size analysis as well as by zeta potential measurements showed the importance of acid/base interactions between AB and CS to achieve an homogeneous dispersion of AB in CS and promote the stabilization of the amorphous state of the drug. These two conditions positively affect drug antimicrobial activity. Indeed, the $(CS:AB)_{SD}$ 1:1 sample, that possessed a good dispersion of AB in the amorphous state, was found to be the best in terms of MIC, also showing a synergy between the two components. Therefore, the $(CS:AB)_{SD}$ 1:1 formulation is promising for a potential application against microbial colonization in different areas, including the food industry and the biomedical field.

Funding

This work was supported by the Sapienza University of Rome.

Conflicts of Interest

The authors declare no conflict of interest.

References

[1] M.S. Butler, A.D. Buss, Natural products — The future scaffolds for novel antibiotics?, Biochem. Pharmacol. 71 (2006) 919–929.

[2] S. Hemaiswarya, A.K. Kruthiventi, M. Doble, Synergism between natural products and antibiotics against infectious diseases, Phytomedicine. 15 (2008) 639–652.

[3] D. Raafat, H-G. Sahl, Chitosan and its antimicrobial potential – a critical literature survey, Microb. Biotechnol. 2 (2009) 186-201.

[4] H.K. No, S.P. Meyers, W.Prinyawiwatkul, Z. Xu, Applications of chitosan for improvement of quality and shelf life of foods: a review, J. Food Sci. 72 (2007) R87-R100.

[5] P.K. Dutta, S. Tripathi, G.K. Mehrotra, J. Dutta, Perspectives for chitosan based antimicrobial films in food applications, Food Chem. 114 (2009) 1173–1182.

[6] S.K. Shukla, A.K. Mishra, O.A. Arotiba, B.B. Mamba, Chitosan-based nanomaterials: a state-of-the-art review, Int. J. Biol. Macromol. 59 (2013) 46-58.

[7] A. Zhang, H. Mu H, W. Zhang, G. Cui, J. Zhu, J. Duan, Chitosan coupling makes microbial biofilms susceptible to antibiotics, Sci. Rep. 28 (2013) 3364.

[8] Y. Liu, P. Ji, H. Lv, Y. Qin, L. Deng, Gentamicin modified chitosan film with improved antibacterial property and cell biocompatibility, Int. J. Biol. Macromol. 98 (2017) 550-556.

[9] Y. Liu, Y. Cai, X. Jiang, J. Wu, X. Le, Molecular interactions, characterization and antimicrobial activity of curcumin–chitosan blend films. Food Hydrocolloid 52 (2016) 564–572.

[10] J. Quesada, E. Sendra, C. Navarro, E, Sayas-Barberá, Antimicrobial active packaging including chitosanfilms with *Thymus vulgaris l.* essential oil forready-to-eat meat. Foods 5 (2016) 57.

[11] R. Hammerschmidt, E.K. Dann, The role of phytoalexins in plant protection. Novartis Found Symp. 223 (1999) 175-87.

[12] I. Ahuja, R. Kissen, A.M. Bones. Phytoalexins in defense against pathogens. Trends Plant Sci. 17(2012) 73-90.

[13] M.A. González, J. Correa-Royero, L. Agudelo, A. Mesa, L. Betancur-Galvis, Synthesis and biological evaluation of abietic acid derivatives, Eur. J. Med. Chem. 44 (2009) 2468-72.

[14] H.J.D. Dorman, S.G. Deans, Antimicrobial agents from plants: antibacterial activity of plant volatile oils, J. Appl. Microbiol. 88 (2000) 308–316.

[15] M. Himejima, K.R. Hobson, T. Otsuka, D.L. Wood, I. Kubo, Antimicrobial terpenes from oleoresin of ponderosa pine tree *Pinus ponderosa*: A defense mechanism against microbial invasion, J. Chem. Ecol. 18 (1992) 1809–1818.

[16] A. Helfenstein, M. Vahermo, D.A. Nawrot, F. Demirci, G. İşcan, S. Krogerus, J. Yli-Kauhaluoma, V.M. Moreira, P. Tammela, Antibacterial profiling of abietane-type diterpenoids, Bioorg. Med.Chem. 25 (2017) 25 132-137.

[17] M.S. Ganewatta, K.P. Miller, S.P. Singleton, P. Mehrpouya-Bahrami, Y.P. Chen, Y. Yan, M. Nagarkatti, P. Nagarkatti, A.W. Decho, C. Tang, Antibacterial and biofilm-disrupting coatings from resin acid-derived materials, Biomacromolecules 16 (2015) 3336-44.

[18] A. Yıldız, M. Değirmencioğlu, Synthesis of silver abietate as an antibacterial agent for textile applications, Bioinorg. Chem. Appl. 2015 (2015) 215354.

[19] M.S. Ganewatta, Y.P. Chen, J. Wang, J. Zhou, J. Ebalunode, M. Nagarkatti, A.W. Decho, C. Tang, Bio-inspired resin acid-derived materials as anti-bacterial resistance agents with unexpected activities, Chem. Sci. 5 (2014) 2011-2016.

[20] C.L.N. Vo, C. Park, B.J. Lee, Current trends and future perspectives of solid dispersions containing poorly water-soluble drugs, Eur. J. Pharm. Biopharm. 85 (2013) 799–813.

[21] B.R. Boles, P.K. Singh, Endogenous oxidative stress produces diversity and adaptability in biofilm communities, Proc. Natl. Acad. Sci. USA 105 (2008) 12503-8.

[22] W. Brand-Williams, M.E. Cuvelier, C. Berset, Use of a free radical method to evaluate antioxidant activity, LWT - Food Sci. Technol. 28 (1995) 25–30.

[23] I. Francolini, A. Piozzi, G. Donelli, Efficacy evaluation of antimicrobial drug-releasing polymer matrices, Methods Mol. Biol. 1147 (2014) 215–25.

[24] V. Taresco, J. Suksiriworapong, I.D. Styliari, R.H. Argent, S.M.E. Swainson, J. Booth, E. Turpin, C.A. Laughton, J.C. Burley, C. Alexander, M.C. Garnett, New N-acyl amino acid-functionalized biodegradable polyesters for pharmaceutical and biomedical applications, RSC Adv. 6 (2016) 109401–109405.

[25] E. Broman, C. Khoo, L.S. Taylor, A comparison of alternative polymer excipients and processing methods for making solid dispersions of a poorly water solubledrug, Int. J. Pharm. 222 (2001) 139-51.

[26] C. Leuner, J. Dressman, Improving drug solubility for oral delivery using solid dispersions, Eur. J. Pharm. Biopharm. 50 (2000) 47–60.

[27] Y. Huang, W.G. Dai, Fundamental aspects of solid dispersion technology for poorly soluble drugs, Acta Pharm. Sin. B. 4 (2014) 18-25.

[28] F. Qian, J. Huang, M.A. Hussain, Drug-polymer solubility and miscibility: Stability consideration and practical challenges in amorphous solid dispersion development, J. Pharm. Sci. 99 (2010) 2941–2947.

[29] I. Francolini, V. Taresco, F. Crisante, A. Martinelli, L. D'Ilario, A. Piozzi, Water soluble usnic acid-polyacrylamide complexes with enhanced antimicrobial activity against *Staphylococcus epidermidis*, Int. J. Mol. Sci. 14 (2013) 7356–7369.

[30] Y. Dong, Y. Ruan, H. Wang, Y. Zhao, D. Bi, Studies on glass transition temperature of chitosan with four techniques, J. Appl. Polym. Sci. 93 (2004) 1553–1558.

[31] P.P. Dhawade, R.N. Jagtap, Characterization of the glass transition temperature of chitosan and its oligomers by temperature modulated differential scanning calorimetry, Adv. Appl. Sci. Res. 3 (2012) 1372-1382.

[32] J. Rotta, E. Minatti, P.L.M. Barreto, Determination of structural and mechanical properties, diffractometry, and thermal analysis of chitosan and hydroxypropylmethylcellulose (HPMC) films plasticized with sorbitol, Ciênc. Tecnol. Aliment. Campinas, 31 (2011) 450-455.

[33] K. Ogura, T. Kanamoto, M. Itoh, H. Miyashiro, K. Tanaka, Dynamic mechanical behavior of

chitin and chitosan, Polym. Bull. 2 (1980) 301-304.

[34] J.S. Ahn, H.K. Choi, C.S. Cho, A novel mucoadhesive polymer prepared by template polymerization of acrylic acid in presence of chitosan, Biomaterials 22 (2001) 923-928.

[35] V. Beltran, N. Salvadò, S. Butì, T. Pradell, Ageing of resin from *Pinus* species assessed by infrared spectroscopy. Anal. Bioanal. Chem. 408 (2016) 4073-4082.

[36] A. Alkhalil, J. Babu Nanubolu, J.C. Burley, Analysis of phase transitions in molecular solids: quantitative assessment of phonon-mode vs intra-molecular spectral data, RSC Adv. 2 (2012) 209-216.

[37] S. Al-Dulaimi, A. Aina, J. Burley, Rapid polymorph screening on milligram quantities of pharmaceutical material using phonon-mode Raman spectroscopy, Cryst. Eng. Comm. 12 (2010) 1038-1040.

[38] M. Pohanka, Role of oxidative stress in infectious disease. A review, Folia Microbiol. 58 (2013) 503-513.

[39] O. Ciofu, B. Riis, T. Pressler, H.E.Poulsen, N. Hoiby, Occurrence of hypermutable *Pseudomonas aeruginosa* in cystic fibrosis patients is associated with the oxidative stress caused by chronic lung inflammation, Antimicrob. Agents Chemother. 49 (2005) 2276-82.

[40] S. Dhall, D. Do, M. Garcia, D.S. Wijesinghe, A. Brandon, J. Kim, A. Sanchez, J. Lyubovitsky, S. Gallagher, E.A. Nothnagel, C.E. Chalfant, R.P. Patel, N. Schiller, M. Martins-Green. A novel model of chronic wounds: importance of redox imbalance and biofilm-forming bacteria for establishment of chronicity, Plos One 9 (2014) e109848.

[41] S. Dhall, D.C. Do, M. Garcia, J. Kim, S.H. Mirebrahim, J. Lyubovitsky, S. Lonardi, E.A. Nothnagel, N. Schiller, M. Martins-Green. Generating and reversing chronic wounds in diabetic mice by manipulating wound redox parameters, J. Diabetes Res. (2014) 562625.

[42] M.T. Yen, J.H. Yang, J.L. Mau, Antioxidant properties of chitosan from crab shells, Carbohydr. Polym. 74 (2008) 840–844.

[43] N. Nenadis, O. Lazaridou, M.Z. Tsimidou, Use of reference compounds in antioxidant activity

assessment, J. Agric. Food Chem. 55 (2007) 5452–5460.

[44] P. Schuler, Natural antioxidants exploited commercially, in: B.J. Hudson (Ed.), Food Antioxidants, Springer, Netherlands, 1990,pp. 99-170.

[45] G.C. Justino, C.F. Correia, L. Mira, R.M. Borges Dos Santos, J.A. Martinho Simões, A.M. Silva, C. Santos, B. Gigante B. Antioxidant activity of a catechol derived from abietic acid. J. Agric. Food Chem, 54 (2006) 342-348.

[46] M. Kong, X.G. Chen, K. Xing, H.J. Park, Antimicrobial properties of chitosan and mode of action: A state of the art review, Int. J. Food Microbiol. 144 (2010) 51–63.

[47] F.J. Aranda, J. Villalaín J, The interaction of abietic acid with phospholipid membranes, Biochim. Biophys. Acta 1327 (1997) 171-180.

[48] L. Wang, C. Hu, L. Shao. The antimicrobial activity of nanoparticles: present situation and prospects for the future. Int. J. Nanomedicine 12 (2017) 1227-1249.

[49] Y. Uemura, I. Moritake, S. Kurihara, T. Nonaka, Preparation of resins having various phosphonium groups and their adsorption and elution behavior for anionic surfactants, J. Appl. Polym. Sci. 72 (1999) 371-378.

Caption to figures

Figure 1. Chemical structure of abietic acid (A) and chitosan (B). In chitosan, m=0.8 and n=0.2.

Figure 2. POM images of AB (A) and solid mixtures $(CS:AB)_{PM}$ 1:1 (B) and $(CS:AB)_{SD}$ 1:1 (C). (A) and (B) images show the phenomenon of light birefringence due to the presence of drug crystalline domains in both the samples. Lack of light birefringence in (C) indicates the amorphous state of the drug in the solid dispersion.

Figure 3. DSC thermogram of abietic acid (A) and chitosan (B), this latter in the first and second cycle of heating.

Figure 4. DSC thermograms of $(CS:AB)_{PM}$ 1:1, 2:1, 4:1 and 6:1 compared to AB.

Figure 5. Enthalpy of melting of $(CS:AB)_{PM}$ as a function of CS:AB molar ratio.

Figure 6. DSC thermograms of $(CS:AB)_{SD}$ 1:1, 2:1, 4:1 and 6:1 compared to AB.

Figure 7. IR spectra of abietic acid (A), chitosan (B), $(CS:AB)_{PM}$ formulations (C) and $(CS:AB)_{SD}$ (D) formulations.

Figure 8. Ratio between the absorbance of the peak at 1554 cm^{-1}($A_{1554,}$ CS) and that of the peak at1690 cm^{-1}($A_{1690,}$ AB) vs CS:AB molar ratio for $(CS:AB)_{PM}$ and $(CS:AB)_{SD}$ formulations.

Figure 9. Raman traces for $(CS:AB)_{PM}$(A) and $(CS:AB)_{SD}$(B) formulations in comparison with pureCS and AB.

Figure 10. Comparison of the MIC values of $(CS:AB)_{PM}$ 1:1 and $(CS/AB)_{SD}$ 1:1.

Figure 11. Inhibition of bacterial growth for $(CS:AB)_{SD}$ 0.5:1, $(CS:AB)_{SD}$1:1 and $(CS:AB)_{SD}$ 6:1 at different concentrations.

Sample (molar ratio)	CS Weight (%)	AB Weight (%)	[CS] mg/ml	[AB] mg/ml	EC_{50} mg/ml
CS	100	0	11	-	**11**
AB	0	100	-	1.65	**1.65**
$(CS:AB)_{SD}$ 0.5:1	20	80	0.104	0.416	**0.52**
$(CS:AB)_{SD}$ 1:1	35	65	0.214	0.396	**0.61**
$(CS:AB)_{SD}$ 6:1	75	25	1.95	0.60	**2.40**

Table 1. Analysis of formulation component antioxidant activity. Amounts of component present in each formulation at the $EC_{50}$are calculated.

Sample (molar ratio)	CS Weight* (%)	AB Weight* (%)	[CS]§ mg/ml	[AB]§ mg/ml	MIC mg/ml
CS	100	0	-	-	**0.5**
AB	0	100	-	-	**0.8**
$(CS/AB)_{SD}$ 0.5:1	20	80	0.20	0.80	**1.0**
$(CS/AB)_{SD}$ 1:1	35	65	0.088	0.162	**0.25**
$(CS/AB)_{SD}$ 6:1	75	25	0.562	0.188	**0.75**

* Weight percentage of each component in the formulation

§ Concentration of each component in correspondence of the MIC

Table 2: MIC values for pure AB, pure CS, and $(CS/AB)_{SD}$ formulations. For each formulation, the weight percentage and the concentration of the two single components in relation to the MIC were calculated.

Sample	Size (nm)	PDI	Zeta Potential (mV)
Chitosan	1000	0.70	+22
$(CS/AB)_{SD}$ 0.5:1	190	0.16	-35
$(CS/AB)_{SD}$ 1:1	370	0.38	-5
$(CS/AB)_{SD}$ 6:1	440	0.67	+11

Table 3. Size, polydispersity index (PDI) and zeta potential of selected $(CS/AB)_{SD}$ samples

Sample	Concentration (expressed as multiplex MIC)ξ	Real concentration (mg/mL)	Hemolysis (%)
CS	5*MIC	2.50	0.04
	1*MIC	0.50	0.01
	0.25*MIC	0.13	0.08
$(CS/AB)_{SD}$ 1:1	5*MIC	1.25	0.15
	1*MIC	0.25	0.06
	0.25*MIC	0.06	0.17
$(CS/AB)_{PM}$ 1:1	5*MIC	5.00	0.08
	1*MIC	1.00	0.18
	0.25*MIC	0.25	0.20
AB	5*MIC	4.00	5.83
	1*MIC	0.80	0.10
	0.25*MIC	0.20	0.10

ξ**MIC values: CS = 0.5 mg/ml; AB = 0.8 mg/ml;** $(CS/AB)_{SD}$ 1/1 = 0.25 mg/ml; $(CS/AB)_{PM}$ 1/1 = 1 mg/ml

Table 4. Hemolysis values for CS, AB, $(CS/AB)_{SD}$ 1:1 and $(CS/AB)_{PM}$ 1:1.

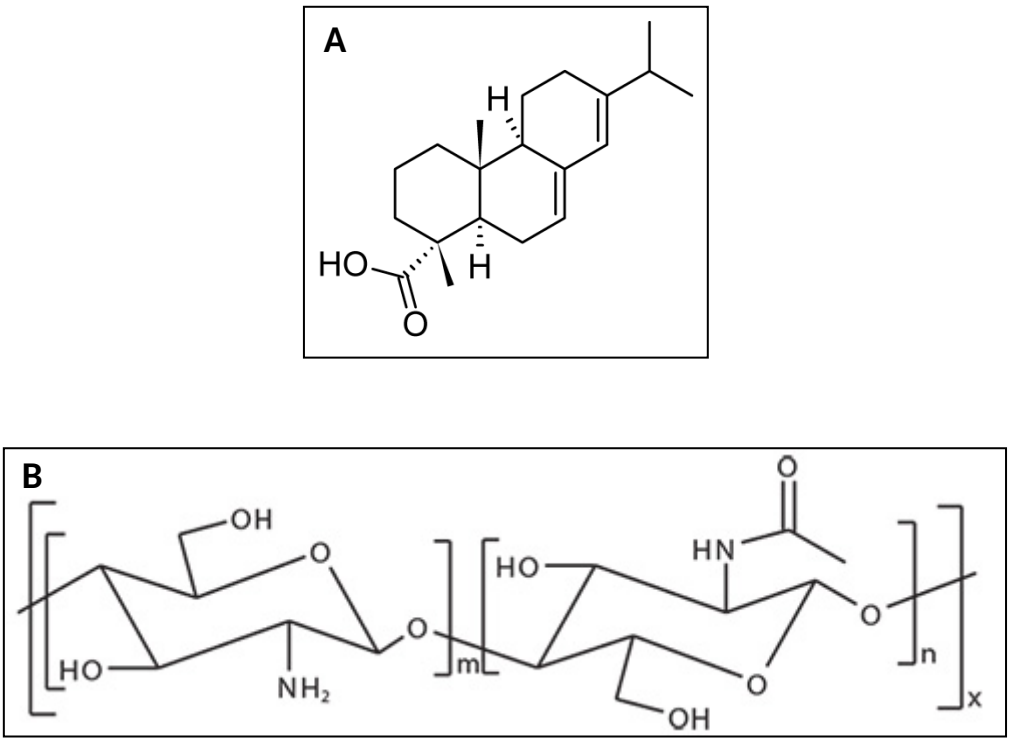

Figure 1. Chemical structure of abietic acid (A) and chitosan (B). In chitosan, m=0.8 and n=0.2.

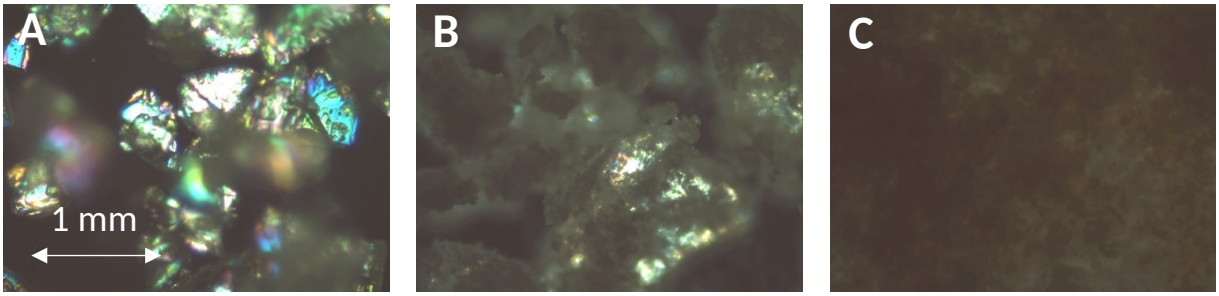

Figure 2. POM images of AB (A) and solid mixtures $(CS:AB)_{PM}$ 1:1 (B) and $(CS:AB)_{SD}$ 1:1 (C). (A) and (B) images show the phenomenon of light birefringence due to the presence of drug crystalline domains in both the samples. Lack of light birefringence in (C) indicates the amorphous state of the drug in the solid dispersion.

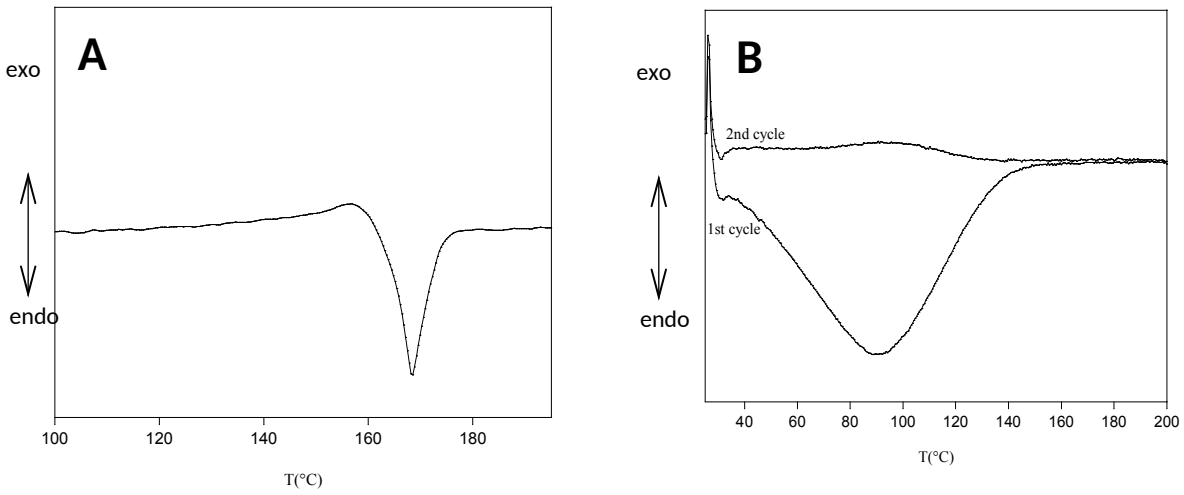

Figure 3. DSC thermogram of abietic acid (A) and chitosan (B), this latter in the first and second cycle of heating.

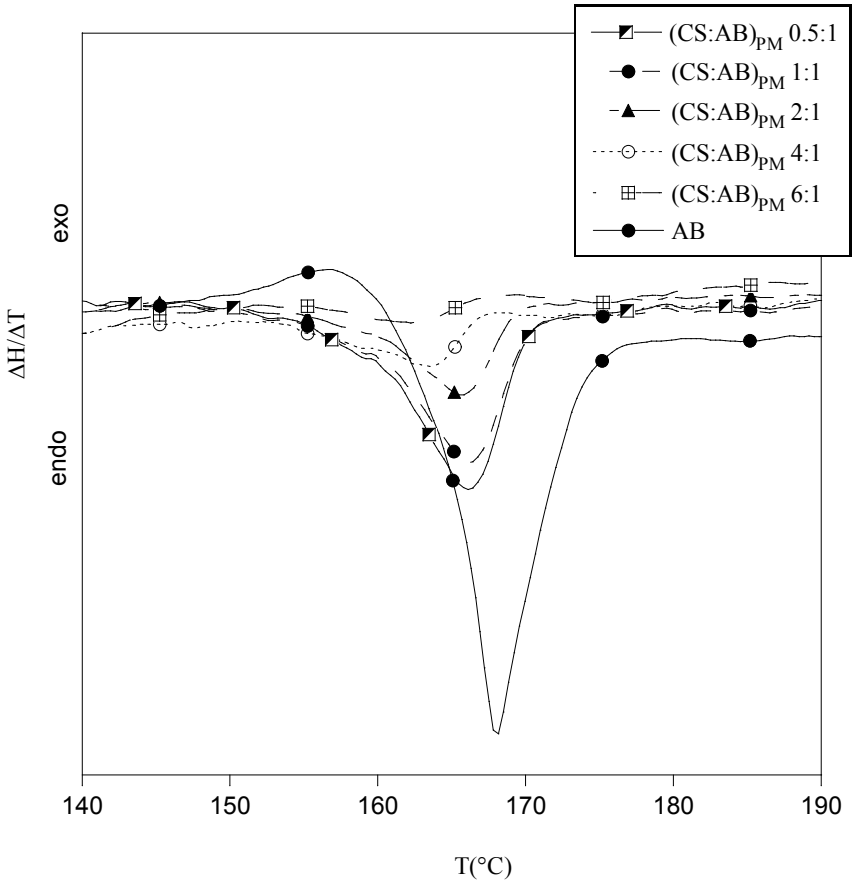

Figure 4. DSC thermograms of $(CS:AB)_{PM}$ 0.5:1, 1:1, 2:1, 4:1 and 6:1 compared to AB.

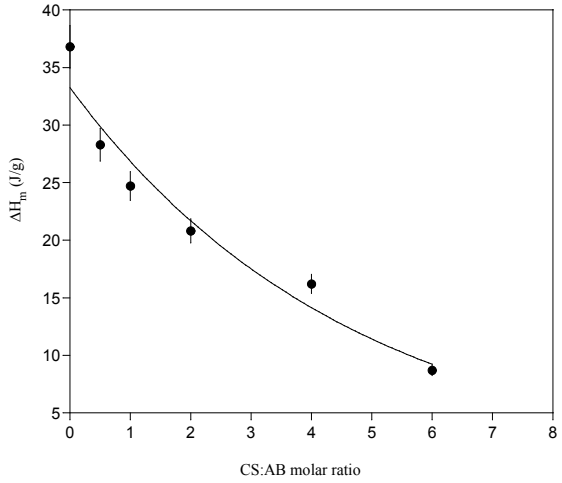

Figure 5. Enthalpy of melting of $(CS:AB)_{PM}$ as a function of CS:AB molar ratio.

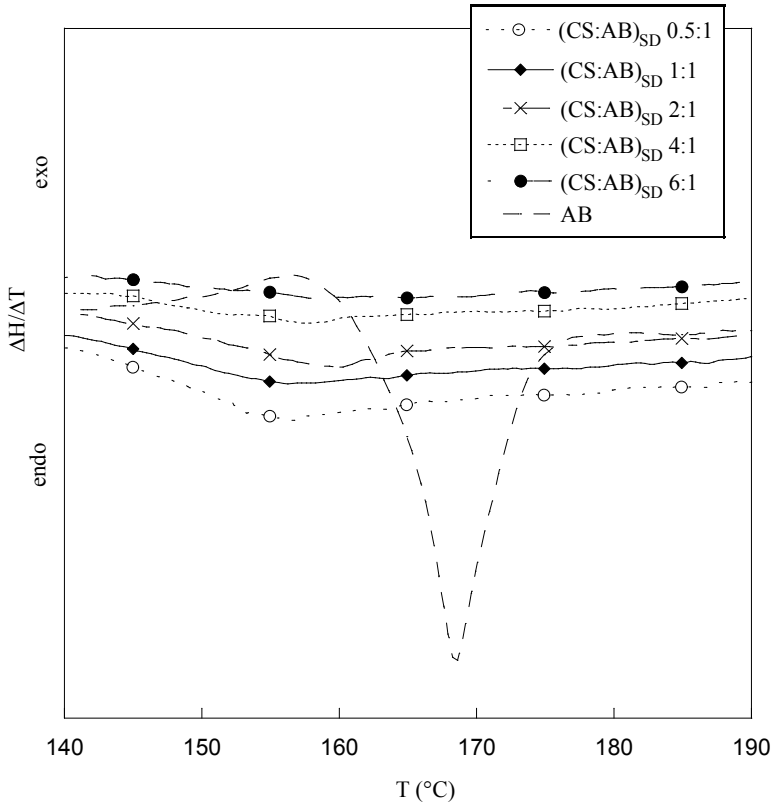

Figure 6. DSC thermograms of $(CS:AB)_{SD}$ 0.5:1, 1:1, 2:1, 4:1 and 6:1 compared to AB.

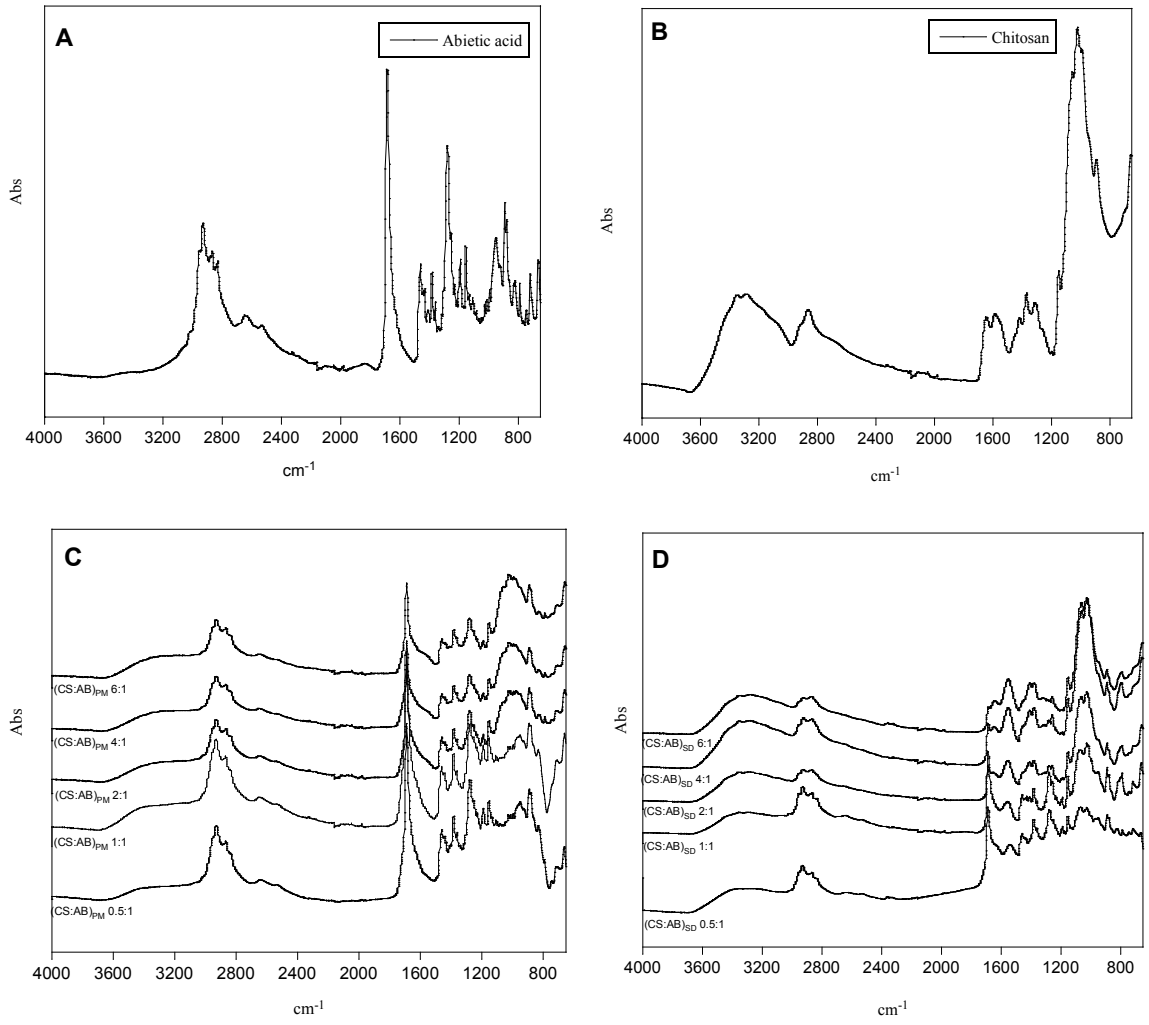

Figure 7. IR spectra of abietic acid (A), chitosan (B), $(CS:AB)_{PM}$ formulations (C) and $(CS:AB)_{SD}$ (D) formulations.

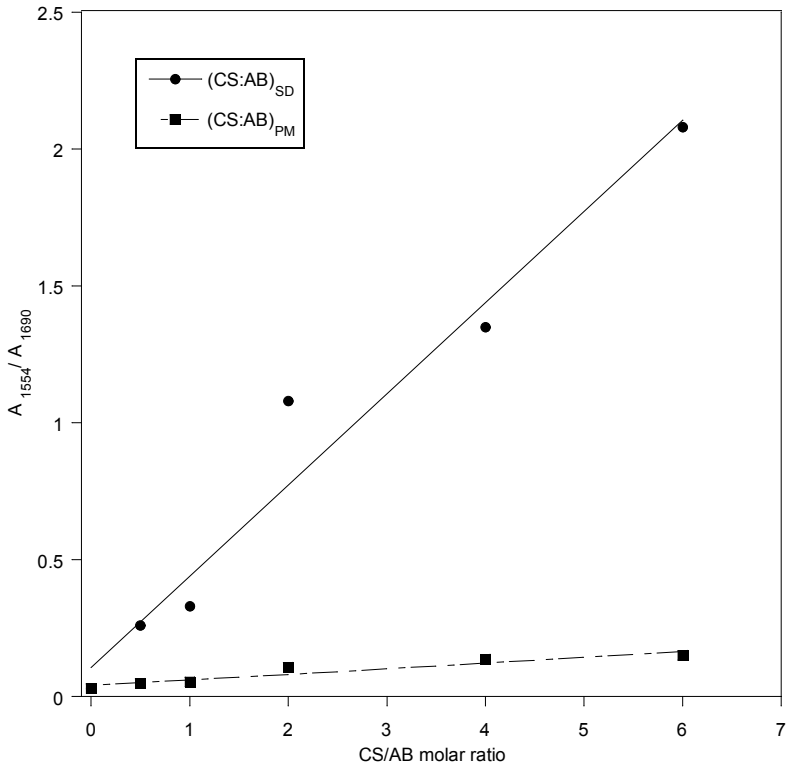

Figure 8. Ratio between the absorbance of the peak at 1554 cm^{-1}($A_{1554,}$ CS) and that of the peak at1690 cm^{-1}($A_{1690,}$ AB) vs CS:AB molar ratio for $(CS:AB)_{PM}$ and $(CS:AB)_{SD}$ formulations.

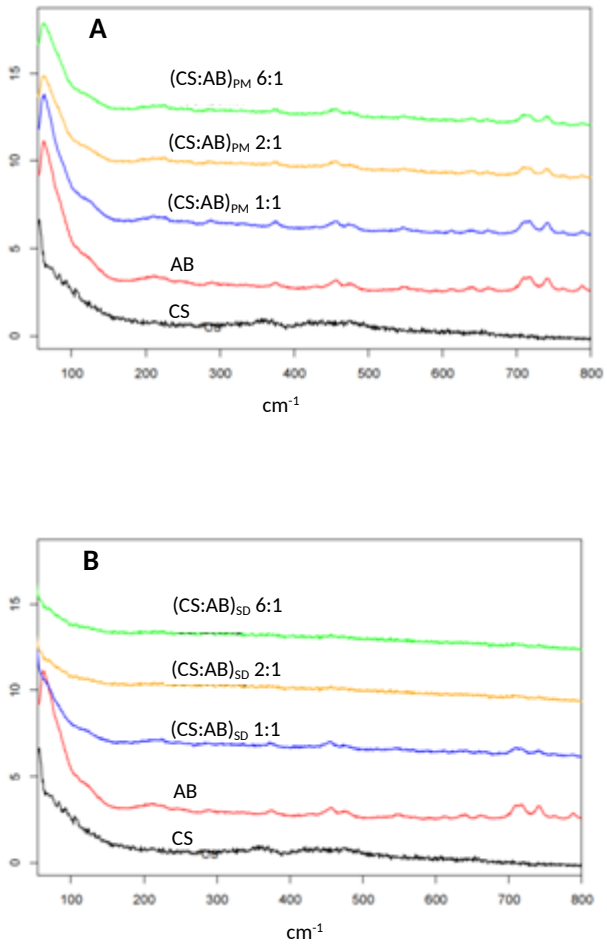

Figure 9. Raman traces for $(CS:AB)_{PM}$ (A) and $(CS:AB)_{SD}$ (B) formulations in comparison with pure CS and AB.

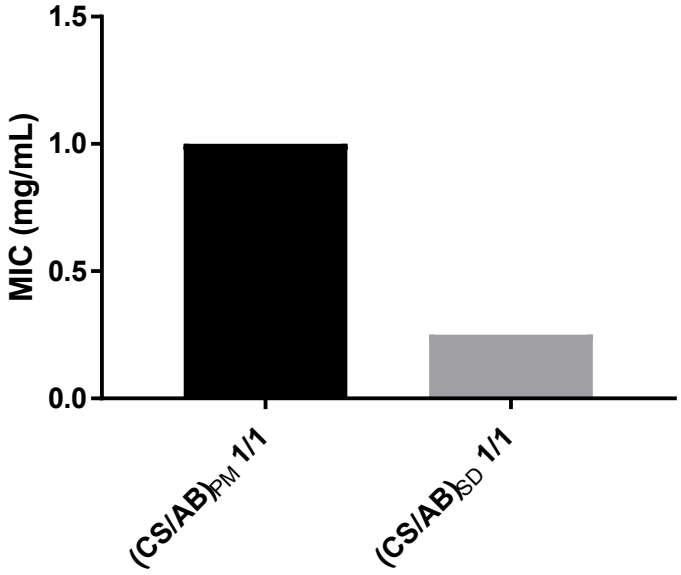

Figure 10. Comparison of the MIC values of $(CS:AB)_{PM}$ 1:1 and $(CS/AB)_{SD}$ 1:1.

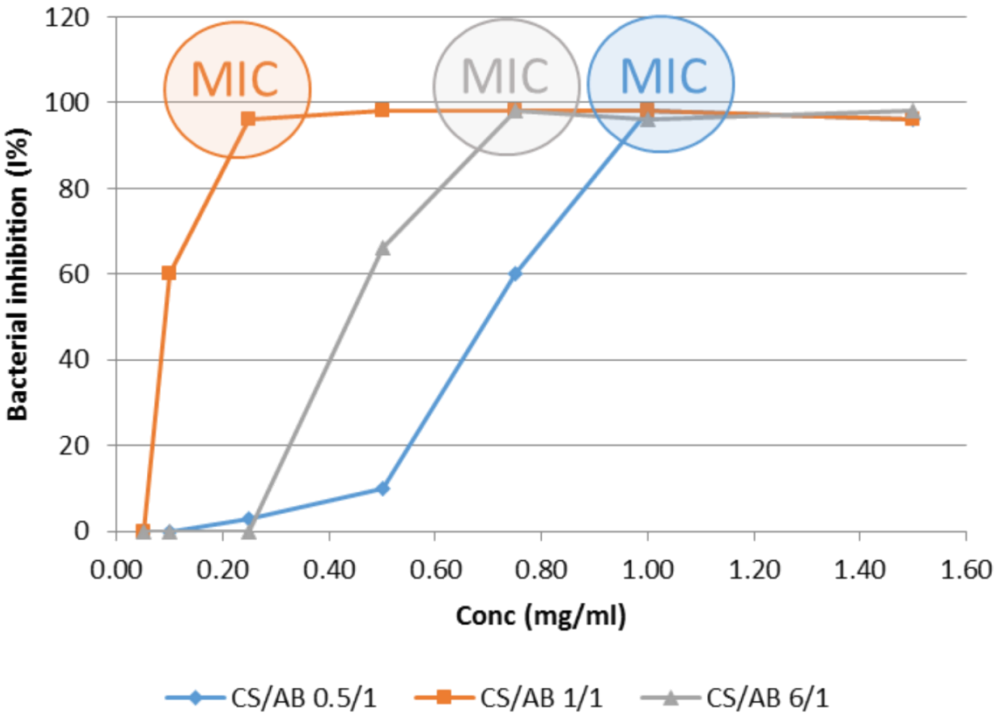

Figure 11. Inhibition of bacterial growth for $(CS:AB)_{SD}$ 0.5:1, $(CS:AB)_{SD}$1:1 and $(CS:AB)_{SD}$ 6:1 at different concentrations.